



# Evaluating the Influence of Multisource Typhoon Precipitation Data on Multiscale Urban Pluvial Flood Modeling

Yi Lu<sup>1,2,3</sup> · Jie Yin<sup>1,4,5</sup> · Dandan Wang<sup>6</sup> · Yuhan Yang<sup>7</sup> · Hui Yu<sup>2,3</sup> · Peiyan Chen<sup>2,3</sup> · Shuai Zhang<sup>2,3</sup>

Accepted: 12 September 2022 / Published online: 10 October 2022  
© The Author(s) 2022

**Abstract** Based on station precipitation observations, radar quantitative precipitation estimates (QPE), and radar fusion data during Typhoon Fitow (2013), the influence of multisource precipitation data on multiscale urban typhoon pluvial flood modeling is studied. Using Shanghai, China, as the study area, a simplified 2D hydrodynamic model is applied to simulations. Combined with actual flood incidents reported by the public and soil moisture data, we perform multiscale verifications and determine the applicability of three precipitation datasets in the modeling. The results are as follows: (1) At the city scale, although QPE have higher spatial resolution, these estimates are lower than station observations. Radar fusion data have both high accuracy and high spatial resolution. For flood depths above 5 cm, the radar fusion precipitation scenario can improve the matching probability by 6%. (2) At the neighborhood scale, the

radar fusion precipitation scenario can effectively mitigate the problems of an uneven spatial distribution of stations and a weak QPE to accurately capture pluvial details. (3) One fixed-point assessment shows that different precipitation data have little influence on the temporal characteristics of the modeling result—all three types of data can accurately reflect flood occurrence times. This work can provide a scientific basis for constructing effective urban pluvial flood monitoring systems.

**Keywords** City and neighborhood scale · Flood validation · Multisource precipitation data · Pluvial flood modeling · Shanghai

## 1 Introduction

The sixth assessment report of the Intergovernmental Panel on Climate Change (IPCC) indicates that the frequency of extreme weather and climate events has increased in the context of climate change, and the resulting flood hazards are very likely to continue to increase in the future (IPCC 2021). Climate change in China shows considerable similarity to global trends. Annual extreme rainfall has significantly increased with a greater magnitude than the global rate, resulting in a higher risk of floods (Ding et al. 2006; Xu et al. 2011; Lai et al. 2020; IPCC 2021; Wu and Wu 2021). Furthermore, China has experienced rapid urban expansion since the reform and opening-up in 1978, and the country's urbanization level (as measured by the percentage of the population living in urban areas) increased from 18% in 1978 to 58.52% in 2017 and is projected to reach approximately 75% at the end of the 2050s (Shi et al. 2006). Sustained and intensive human activities have weakened the ability of cities to respond to climate change and the

✉ Jie Yin  
jyin@geo.ecnu.edu.cn

- <sup>1</sup> Key Laboratory of Geographic Information Science (Ministry of Education), East China Normal University, Shanghai 200241, China
- <sup>2</sup> Shanghai Typhoon Institute, China Meteorological Administration, Shanghai 200030, China
- <sup>3</sup> Key Laboratory of Numerical Modeling for Tropical Cyclone of China Meteorological Administration, Shanghai 20030, China
- <sup>4</sup> Institute of Eco-Chongming, East China Normal University, Shanghai 202162, China
- <sup>5</sup> Research Center for China Administrative Division, East China Normal University, Shanghai 202162, China
- <sup>6</sup> National Disaster Reduction Center of China, Beijing 100124, China
- <sup>7</sup> State Key Laboratory of Estuarine and Coastal Research, East China Normal University, Shanghai, China

self-regulation of the social-ecological systems. Owing to a significant increase in impervious surfaces, increased risk exposure in urban areas, and poor drainage capacity, ongoing urbanization has further amplified the adverse effects of rainstorm and pluvial flood hazards. Among all these hazards, pluvial floods caused by tropical cyclones (TCs) are among the most serious and are responsible for significant property damage and loss of life in China. Coastal megacities, as national economic centers, are more seriously affected by typhoon pluvial floods than inland and less developed area due to their specific geographical location and dense population and wealth (Chen et al. 2012; Chen et al. 2017; Zhang and Chen 2019). Typhoon pluvial flooding has become one of the major challenges for coastal cities in China, as it is worldwide.

Recently, the construction of urban flood models has achieved great progress, developing from traditional hydrological methods to one/two-dimensional (1D/2D) coupled hydraulic methods. For urban pluvial flooding, representative models such as the storm water management model (SWMM),<sup>1</sup> storage treatment overflow and runoff model (STORM),<sup>2</sup> MIKE-Urban,<sup>3</sup> InfoWorks CS,<sup>4</sup> hydrologic engineering center-hydrologic modeling system (HEC-HMS),<sup>5</sup> DigitalWater,<sup>6</sup> and integrated flood modeling system (IFMS) Urban<sup>7</sup> models have been employed (Yin et al. 2015; Song and Xu 2019). Based on these models, a large number of studies have carried out urban flood modeling by focusing on rainfall runoff processes in cities (Wang and Altunkaynak 2012; Bisht et al. 2016; Li et al. 2016). However, such models mostly use irregular grids to construct complex urban topographical elevations, whose modeling schemes are complicated and modeling results are not ideal (Yin et al. 2015). To overcome such shortcomings, researchers have established high-resolution, GIS-based urban flood models, such as Lis-Flood and FloodMap in the United Kingdom. These models combine a high-resolution digital elevation model (for example, LiDAR-DSM<sup>8</sup>), an urban hydrological model (for example, evaporation, infiltration, and so on), a

1D storm sewer drainage network, and a river hydrodynamic model with the 2D hydrodynamic model (from a diffusion-wave model to a simplified inertial model, and then to a full hydrodynamic model). These models, with their simple schemes, provide ideal simulations (Bates and De Roo 2000; Bates et al. 2010; Yu and Coulthard 2015).

Previous studies indicated that the accuracy of urban flood modeling is closely related to the spatial and temporal resolutions of the input precipitation data (Ly et al. 2013; Sirisena et al. 2018). At present, most studies of urban flood modeling have focused on seasonal rainfall. The input precipitation data are often obtained from station observations, radar or satellites estimates, or results calculated by rainstorm intensity formulas (Gigović et al. 2017; Yoon and Lee 2017; Tang et al. 2018). For seasonal rainfall or rainfall progress, radar- or satellite-estimated precipitation data, with their high spatial and temporal coverage, are more suitable for urban flood modeling (Abro et al. 2021; Chao et al. 2021). For TC rainfall, satellite-estimated precipitation often seriously underestimates the rain intensity (Chen et al. 2013), resulting in a poor performance of flood modeling based on this data source. If decision makers use flood inundation simulations as a reference, the subsequent disaster emergency response and management may be greatly affected (Mosaffa et al. 2020). For example, on 20 July 2021, a severe rainstorm and flood hazard occurred in Zhengzhou City, Henan Province. Affected by the long-distance water vapor transport of 2021 Severe Typhoon In-Fa, the hourly precipitation at Zhengzhou National Weather Station reached 201.9 mm (16:00 to 17:00 on 20 July), breaking the historical extreme value of hourly precipitation in the Chinese mainland. For those who were in charge of the emergency response deployment, the hourly precipitation had far exceeded their subjective understanding of the rainfall in northern China. Consequently, the emergency response was not timely, resulting in 380 deaths and RMB 40.9 billion yuan (USD 7.7 billion) in direct economic losses. In addition, compared with other regions in the world, there are few studies on the influence of typhoon precipitation data on urban pluvial flood modeling in China thus far. Therefore, carrying out this research has important scientific and practical significance.

Fully understanding the applicability of precipitation data with different temporal and spatial resolutions and observation sources in urban flood modeling is fundamental to urban typhoon pluvial flood prediction, early warning, and emergency management. Shanghai, a coastal megacity in China, was chosen as the study site in this research. Based on the automatic meteorological station observations, radar quantitative precipitation estimates (QPE), and radar fusion data during the impact period of the 2013 Typhoon Fitow, the applicability of these three types of precipitation data in urban typhoon pluvial flood modeling is studied. Moreover,

<sup>1</sup> <https://www.epa.gov/water-research/storm-water-management-model-swmm>.

<sup>2</sup> <https://www.sieker.de/en/software/software-gis/product/storm-software-for-modelling-of-water-management-systems-44.html>.

<sup>3</sup> <https://www.dhigroup.com/mikebydhi/products/mike-urban>.

<sup>4</sup> <https://www.innovyze.com/en-us/blog/retirement-of-infoworks-cs-is-now-complete>.

<sup>5</sup> <https://www.hec.usace.army.mil/software/heh-hms/>.

<sup>6</sup> <https://www.evoqua.com/en/evoqua/products--services/digital-water/>.

<sup>7</sup> <http://cdr.iwhr.com/fhkhjzxx/kycg/jscg/zycp/webinfo/2020/07/1586521667705828.htm>.

<sup>8</sup> <https://www.data.gov.uk/dataset/f0db0249-f17b-4036-9e65-309148c97ce4/national-lidar-programme>.

pluvial flood modeling is performed at the city, neighborhood, and fixed-point scales by adopting a 2D hydrodynamic model, namely FloodMap-Hydroinundation2D. Then, the influence of these multisource precipitation data on multiscale urban typhoon pluvial flood modeling is revealed, which can serve as a scientific reference for Shanghai to build an effective urban typhoon pluvial flood prediction and early warning system. Section 2 describes the materials and methods, Sect. 3 presents the results and discussion, and conclusions and some recommendations for further research are discussed in Sect. 4.

## 2 Materials and Methods

The following subsections present brief introductions to the study area, the 2013 Typhoon Fitow, the employed datasets, data sources, and their properties, followed by the 2D hydrodynamic model adopted in urban pluvial flood simulation.

### 2.1 Study Area and Typhoon Fitow

Shanghai Municipality lies on part of the alluvial plain of the Yangtze River Delta, with a total area of 6,340 km<sup>2</sup>. It has a population of 24.87 million (2020).<sup>9</sup> The city lies on the west bank of the Pacific Ocean, bordering Jiangsu and Zhejiang Provinces, which are highly exposed to typhoon-induced hazards (Fig. 1). Typhoon rainstorms, storm surges, astronomical spring tides, and upstream floods often occur in this region. In addition, the whole city generally lies on very flat, low-lying land, with an average altitude of approximately 3–4 m above the Wusong Datum, resulting in a low drainage capacity. Because of sustained and intensive human activities, natural river channels in the city center have been significantly reduced, while impervious surfaces have rapidly increased. Thus, urban rainfall runoff has been increasing (Wu et al. 2012; Lin 2014; Quan 2021).

Typhoon Fitow was generated in the ocean east of the Philippines on 30 September 2013 and then achieved typhoon strength on 4 October. Fitow made landfall at 1715 UTC on 7 October in the city of Fuding, Fujian Province, with maximum sustained winds near 42 m/s. It then rapidly weakened into a tropical depression (Fig. 1). Fitow affected 12.16 million people in East China (Shanghai Typhoon Institute 2014), and the direct economic losses reached RMB 63.14 billion yuan (USD 9.9 billion). In 6–9 October, a TC-caused rainstorm occurred in Shanghai, the northern coast of Zhejiang and southeastern Jiangsu Provinces, locally reaching extremely heavy levels that were rarely seen historically (Wang, Xu, et al. 2017; Wang, Yu, et al. 2017). In

Shanghai, owing to the TC rainstorm, traffic was stopped throughout the city. Over 900 communities, 97 roads, and 100,000 households and shops were flooded.

### 2.2 Data Availability and Processing

The following subsections introduce the basic data and multisource precipitation data as well as present the three main processes of the study including flooding points processing, modeling flood inundation, and evaluating pluvial flood simulation.

#### 2.2.1 Basic Data

**2.2.1.1 Topographic Data** At the city scale, a city-wide digital elevation model constructed from 0.5 m topographic contours is used, with a grid cell resolution of 50 m (Yin et al. 2013). At the neighborhood scale, a standard LiDAR digital surface model (DSM) with a gridded resolution of 2 m was obtained from the Shanghai Surveying and Mapping Institute,<sup>10</sup> representing detailed surface features (Yin et al. 2020).

**2.2.1.2 Flooding Points** These data points identify flood incidents reported by the public during Fitow, provided by the Shanghai Meteorological Service, including date, coordinates, and event description, among other fields (Shi et al. 2014). This dataset contains 4,500 flooding records (road flood, house inundation, and so on) in Shanghai. Among these records, multiple incidents may be reported by different people at one location. There are a total of 2,975 flooding points in the city, 564 in the central area, and 34 in the neighborhood we studied as shown in Fig. 1.

**2.2.1.3 Soil Moisture Data** These data are obtained from the Shanghai Songjiang Meteorological Service,<sup>11</sup> including the 10 m soil relative humidity, volume water content, and weight water content. The study period is from 4 to 9 October 2013, and the temporal resolution is hourly. The meteorological station observations mainly include temperature, humidity, air pressure, wind, precipitation, and visibility. The soil moisture data used in this study are agrometeorological observations. Different from the extensive distribution of meteorological stations, there were only few agrometeorological stations around 2010. According to the National Statistical Yearbook (2014),<sup>12</sup> Wu et al. (2016), and Wang et al. (2018), in 2013, there was only one long-term operational agrometeorological station in Shanghai,

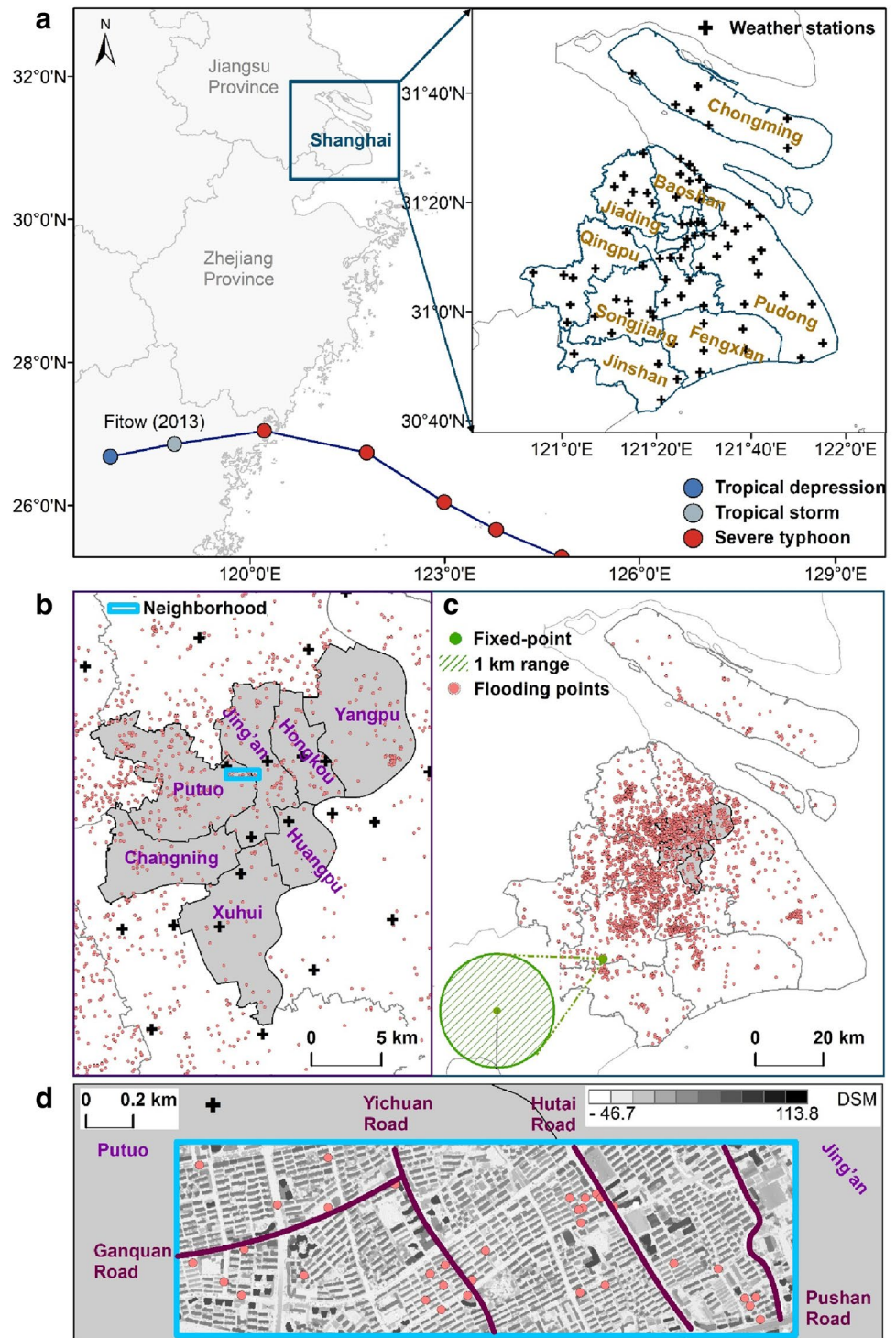
<sup>9</sup> <https://tjj.sh.gov.cn/tjnjrktjn2020e.htm>.

<sup>10</sup> <https://www.shsmi.cn/>.

<sup>11</sup> <http://sh.cma.gov.cn/sj/>.

<sup>12</sup> <http://www.stats.gov.cn/tjsj/ndsj/2014/indexch.htm>.

**Fig. 1** **a** Location of Shanghai Municipality, distribution of weather stations, and the best track and intensity of Fitow (2013); **b** locations of central districts and the studied neighborhood; **c** the fixed-point and the flooding points reported by the public; **d** the studied neighborhood (from Ganquan Road in the west to Pushan Road in the east). *DSM* digital surface model



which is the fixed-point given in Fig. 1. The site is located in Songjiang District, and its data are continuous. According to the requirements of agrometeorological station selection, the observations should be representative of the natural soil moisture status in the area. Therefore, the data of this one

fixed-point are used to analyze the temporal characteristics of inundations. Using the 1 km radius range of the fixed-point as the study area, we compare the soil humidity before and after the typhoon rainfall and the start time of inundation under the three rainfall scenarios.

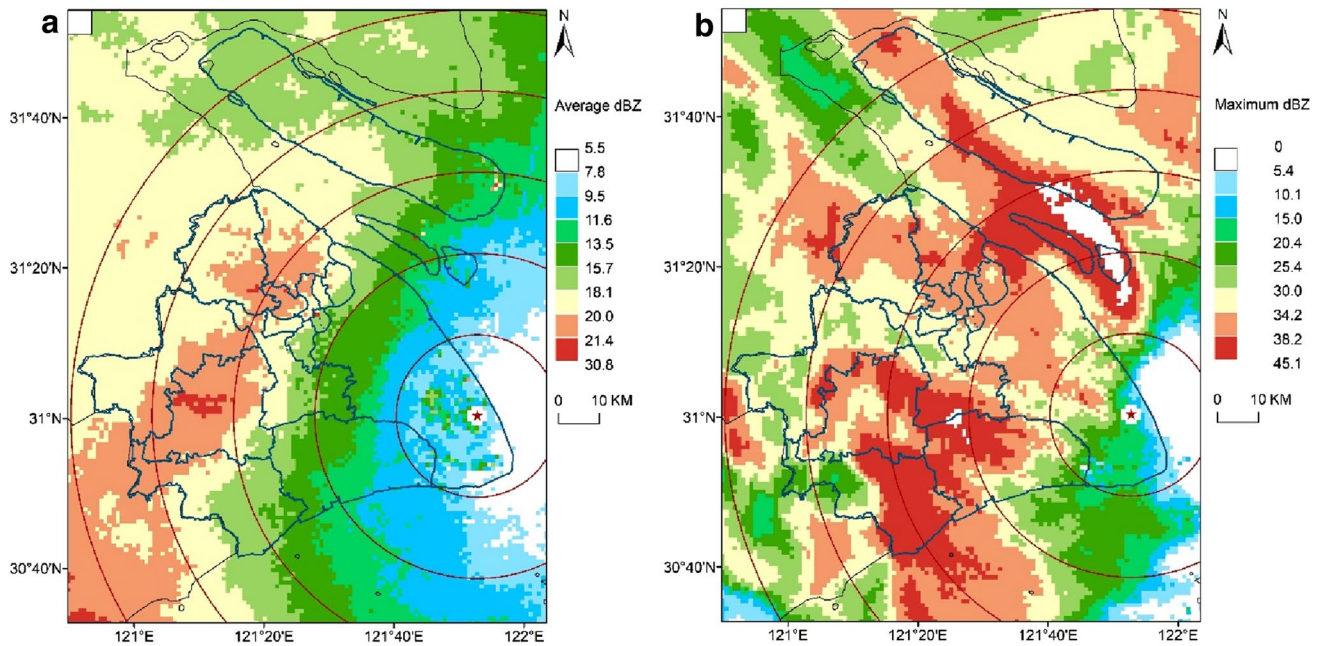


**Fig. 2** The average (a) and strongest (b) reflectivity of the Nanhui Radar Station (Z9210, asterisk mark) during Fitow (2013) at 1500 UTC 7 October 2013.  $\text{dBZ} = 10\log(Z)$

### 2.2.2 Multisource Typhoon Precipitation Data

Three sets of typhoon precipitation data are obtained from the information center of the Shanghai Meteorological Service, including station observations, QPE, and radar fusion data. The period that the three datasets cover is from 6 to 8 October 2013, and the temporal resolution is hourly.

Station observations are measured by 81 automatic weather stations. According to the statistics, in 2017, more than 260 automatic weather stations existed in Shanghai, with the spatial distance of 4 km in the central area and 5–6 km in other districts (Gao et al. 2017). Therefore, the stations were unevenly distributed throughout the city, and the spatial resolution is much lower than that of radar products.

The processing of QPE is based on the relationship between radar reflectivity and rainfall intensity, which enables precipitation to be estimated from radar base data (Zhang et al. 2001). Thus, we extract the average and strongest reflectivity of the Nanhui radar station during Fitow from which the heavy rainfall center can be inferred. As shown in Fig. 2, the center is mainly located in southwestern Shanghai. Wen et al. (2018) investigated the relationship between the drop size distribution and drop shape relation of TCs that made landfall in China. They found that due to the high concentration of small and medium-sized raindrops, previous  $Z$  (reflectivity factor)– $R$  (rain rate) relationships for typhoon systems over various regions tended to underestimate the TC rainfall in China. Thus, a new relationship was presented by Wen et al. (2018) for TCs in China. In our study, by applying

this research result, a QPE dataset is obtained. Finally, radar fusion data with a 1 km resolution are processed by the information center of the Shanghai Meteorological Service, which are directly obtained and applied in this study.

The three sets of precipitation data are compared. As shown in Fig. 3, the QPE before the modification of Wen et al. (2018) is noted as the “original  $Z$ – $R$ ” and the QPE modified by Wen et al. (2018) is noted as the “new  $Z$ – $R$ .” The equation of the “new  $Z$ – $R$ ” is  $Z = 147.28R^{1.38}$  (Wen et al. 2018). The radar fusion data are found to be most consistent with the station observations, and the two sets of QPE are both weak to varying degrees, especially under the “original  $Z$ – $R$ ” relationship. Therefore, for the remainder of this study, only the QPE under the “new  $Z$ – $R$ ” is used.

### 2.2.3 Flooding Points Processing

There are 4,500 records in the original data of flooding points in the city. Most of these incident records were textual descriptions reported by the public, such as the depth of the water to the ankle, and so on. This kind of text descriptions is difficult to use for quantitative comparison and verification. Therefore, with reference to the quantitative standards given in Table 1, the textual messages of 34 flooding points in the study neighborhood are translated to determine the inundation depth. Although we cannot obtain the actual height of all persons who reported, according to the identity card numbers in this data set, we can confirm that they are all

**Fig. 3** Comparison of total precipitation data from different sources during Fitow (2013). Left: intensity of precipitation; right: frequencies

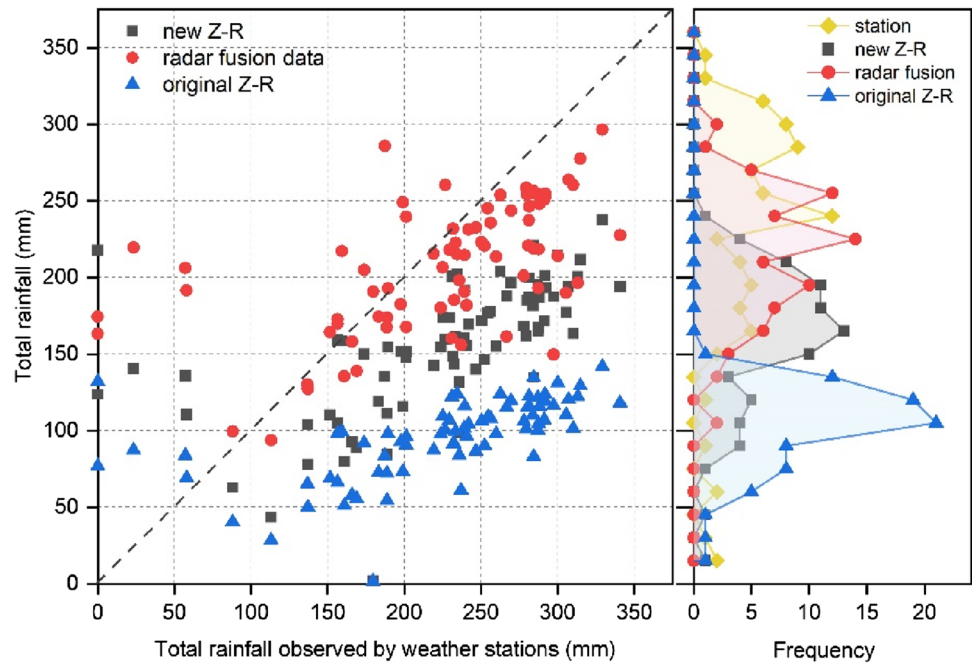


**Table 1** Standards of inundation depths from flood incidents reported by the public Source Shanghai Meteorological Service (<http://sh.cma.gov.cn/>)

Standards	Defined inundation depth (cm)
Inundation to feet	5
Inundation to ankle	15
Inundation to half tire	28
Inundation below shins	30
Inundation about to shins	35
Car flooded or inundation over chassis	40
Inundation to shins	40
Inundation about to knee	45
Inundation to knee	50
Inundation over knee	60
Inundation to thigh	70
Inundation over thigh	80
No explicit statement	Missing data
Actual observed depth	Corrected to cm accuracy

adults. Therefore, these standards are roughly set according to the average height and proportion of adults. There may be some deviations, but in order to meet the needs of quantitative evaluation, simplified considerations are made here.

### 2.2.4 Flood Inundation Modeling

The FloodMap-HydroInundation2D model, which couples hydrological processes (for example, infiltration, evapotranspiration, and drainage) with a 2D hydrodynamic model, is

employed to derive typhoon rainstorm flood inundation for each scenario. The flood routing has the same structure as the inertial model of Bates et al. (2010), but uses a slightly different approach to calculate the time step. The convective acceleration term in the Saint-Venant equation is neglected, and the main governing equation on the regular grid (Yu and Coulthard 2015) becomes:

$$q_{t+\Delta t} = \frac{q_t - gh_t\Delta t(\frac{\partial(h_t+z)}{\partial x})}{(1 + gh_t\Delta t n^2 q_t / h_t^{10/3})} \tag{1}$$

where  $q_t$  is the flow at time  $t$ ,  $\Delta t$  is the time step,  $g$  is the acceleration due to gravity,  $z$  is the bed elevation,  $h_t$  is the water depth at time  $t$ , and  $n$  is Manning’s roughness coefficient.

Infiltration over saturation is represented by the widely used Green-Ampt equation as follows:

$$f(t) = K_s(\frac{\varphi_f + h_o}{z_f} + 1) \tag{2}$$

where  $K_s$  is the hydraulic conductivity of the soil at field saturation,  $h_o$  is the ponding water on the soil surface,  $\varphi_f$  is the capillary potential across the wetting front, and  $z_f$  is the cumulative depth of infiltration.

Daily potential evapotranspiration is calculated by using a simple seasonal sine curve (Calder et al. 1983), and the equation is:

$$E_p = \overline{E_p}[1 + \sin(\frac{360i}{365} - 90)] \tag{3}$$

where  $\overline{E_p}$  is the mean daily potential evapotranspiration and  $i$  is the day of the year.

The model can also be coupled with the SWMM drainage network model or any generalized design drainage capacity model (for example, the Nash model) to calculate the runoff loss of urban rainfall drainage systems. As the extreme storm tide level induced by Fitow approaches or even exceeds the urban land elevation, the drainage system cannot operate normally and discharge water into the Huangpu River and surrounding rivers. Thus, the urban drainage is closed in this flood model. In addition, according to previous studies, empirically-based optimal parameters (that is, a hydraulic conductivity value of 0.001 m/h and a roughness value of 0.06) are used for urban typhoon pluvial flood modeling (Yin et al. 2016).

### 2.2.5 Evaluation of Pluvial Flood Simulation

The performance of multiscale pluvial flood simulations using three different precipitation datasets is comprehensively evaluated by the root mean square error (RMSE) and probability of detection (POD). Among them, the RMSE reflects the range of inundation depth deviation, which can measure the stability of the simulation. The POD represents the probability of a simulated flood matching actual flooding points. The formulas of these two indices are as follows:

$$RMSE = \sqrt{\frac{\sum_{i=1}^N (Simulate_i - Gauge_i)^2}{N}} \quad (4)$$

$$POD = \frac{H}{H + M} \quad (5)$$

where  $N$  is the sample size,  $Simulate_i$  represents the simulated inundation depth, and  $Gauge_i$  is the observed inundation depth, which is obtained from the flood incidents reported by the public. When the simulated points are actually inundated,  $H$  (Hit) indicates that the simulated inundation depth is greater than or equal to the set threshold.  $M$  (Miss) has the opposite meaning, indicating that the simulated inundation depth is less than the set threshold.

## 3 Results and Discussion

Using the three sets of typhoon precipitation data and flooding point data, this section compares and evaluates the inundation simulation results at the city and neighborhood scales. In addition, temporal characteristics of pluvial flood modeling are also discussed.

### 3.1 Pluvial Flood Simulation at the City Scale

By comparing the spatial distribution of the total precipitation during Fitow, the rainfall intensity and distribution of the station observations and the radar fusion data are found to be the most similar, followed by the QPE. Limited by the spatial resolution of the weather stations, the interpolated total precipitation data are slightly overestimated in the southeastern corner of Shanghai, where weather stations are sparse. Therefore, to a certain extent, radar fusion data or QPE with a 1 km resolution can improve the spatial resolution and accuracy of weather station data, which is helpful for providing refined input for urban typhoon pluvial flood simulation.

The three datasets of total precipitation are applied as boundary conditions of the FloodMap-HydroInundation2D model, and the city-scale simulated results with a 50 m resolution are shown in Fig. 4. The actual distribution of the flooding points in the city has been indicated in Fig. 1. Due to the extensive flat and low-lying land in Shanghai, the spatial distribution of the inundation is basically consistent with the heavy rainfall and flooding points. The maximum inundation mainly occurs in the relatively low-lying areas of western Shanghai. Using station observations and radar fusion data (Fig. 4d, e), the inundation simulation results (extent and depth) are relatively close, with significant inundation (20–60 cm) mainly occurring in the western regions of Shanghai. In contrast, the simulation using the QPE (Fig. 4f) is slightly weaker, with an approximately 10–20 cm difference from the other two simulations, especially in the regions without heavy rainfall. The center of significant simulated inundation is basically consistent with the concentrated area of flooding points. In addition, it should be noted that these observed flooding points mainly depend on the report frequency, which is not only related to rainfall intensity and inundation but also is affected by subjective and objective factors such as population density, underlying surface conditions, and awareness of threat (that is, the residents are aware that they can report flooding to the police). Because of certain uncertainties and deviations, these flooding points can be used only as supplementary methods for flooding verification.

Figure 5 displays a comparison of the inundation areas (divided into six inundation depths) in the seven central urban areas of Shanghai under the scenarios of station observations, radar fusion data, and QPE, which are represented as  $S_A$ ,  $S_B$ , and  $S_C$ , respectively. These scenarios are defined as those inundation areas with a depth above 20 cm revealed in the station observation, radar fusion data, and QPE scenarios, respectively. In addition, the specific geographical locations of all districts are shown in Fig. 1. Except in the Yangpu and Hongkou Districts, the proportion of inundation

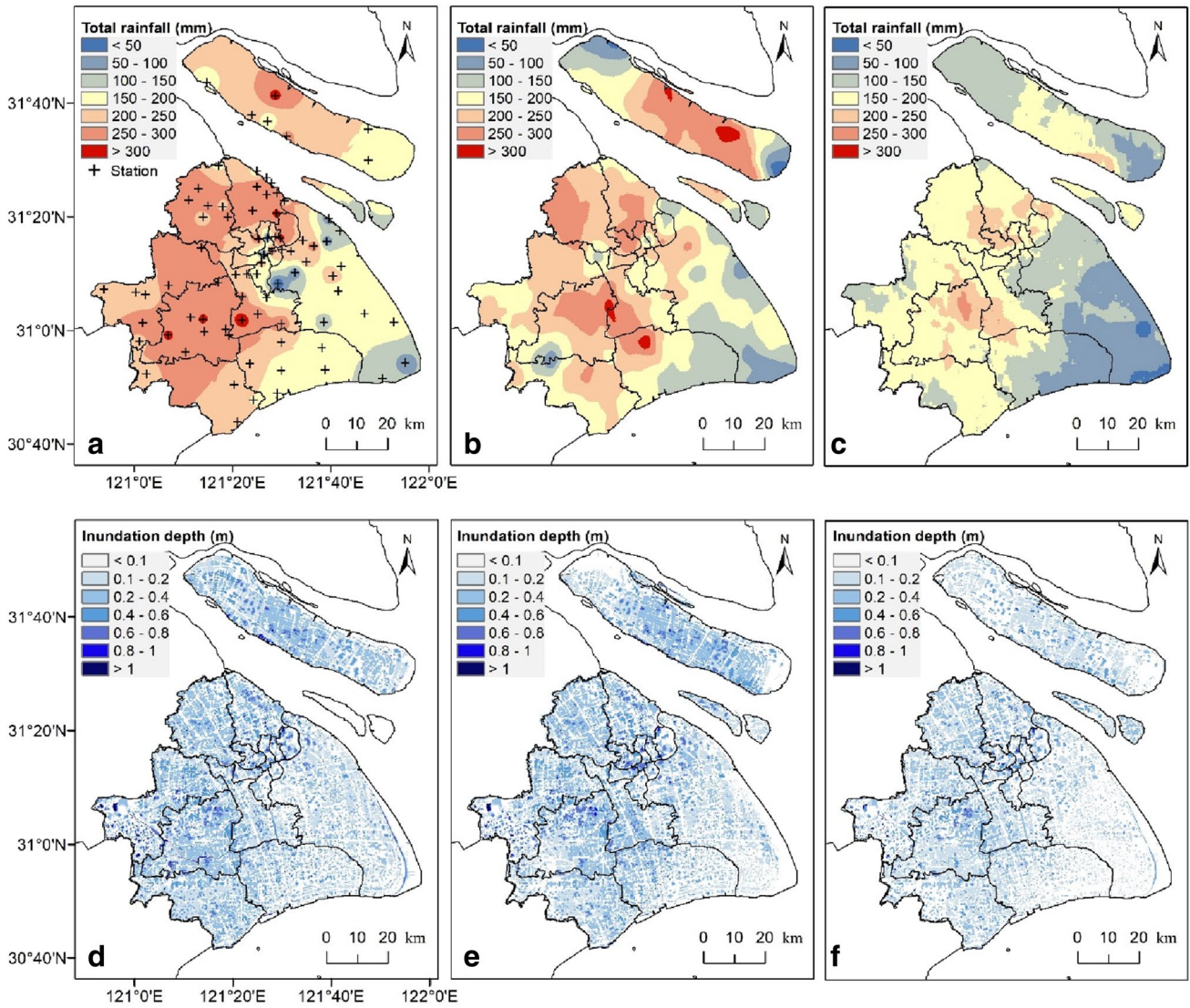


**Fig. 4** Total precipitation and pluvial flood inundation maps under three different rainfall scenarios during Fitow (2013). **a, d** scenario of station observations; **b, e** scenario of radar fusion data; **c, f** scenario of QPE

(depth above 20 cm) areas is the highest under the radar fusion data scenario in all the districts, that is,  $S_C < S_A < S_B$ . Specifically,  $S_B$  in Huangpu District accounts for approximately 43% of the whole district, while  $S_C$  accounts for only 21%. Similarly,  $S_B$  and  $S_C$  account for 53% and 33% of the total area in Jing'an District, 52% and 32% in Putuo District, 39% and 27% in Changning District, and 31% and 23% in Xuhui District, respectively. The difference between  $S_B$  and  $S_C$  is approximately 8–22%, which is consistent with the inundation distribution characteristics (Fig. 4). In the central area of Shanghai, Putuo District has the largest number of flooding points, with more than 200. The number of flooding points in Jing'an and Yangpu Districts take the second place, about 100 respectively. However, there are few flooding points in Xuhui District, whose area is similar to that

of Yangpu District. This may be closely related to the high proportion of inundation area with depths above 20 cm and the relatively low topography in Yangpu and Putuo districts.

To quantitatively analyze the influence of multisource typhoon precipitation data on city-scale urban pluvial flood modeling, the PODs under the three precipitation scenarios are calculated (Table 2). At all flooding points with flooding reports, simulated inundations with depths above 0 cm are presented in all three scenarios. When the observed inundation depth is above 2 cm, the POD under the radar fusion data scenario is the highest, at up to 80%, while that under the scenarios of station observations and QPE are 77% and 75%, respectively. When the observed inundation depth is above 5 cm, in contrast to the QPE scenario, the POD under the radar fusion data scenario can improve by 6%. Therefore,

**Fig. 5** Inundation extent and number of flooding points under different depths in the central area of Shanghai during Fitow (2013). **A** Scenario of station observations; **B** scenario of radar fusion data; **C** scenario of QPE; Upper graph: the numbers of flooding points in each district; Lower graph: inundation extents under different depths; White % figures: proportion of inundation area with depth below 20 cm

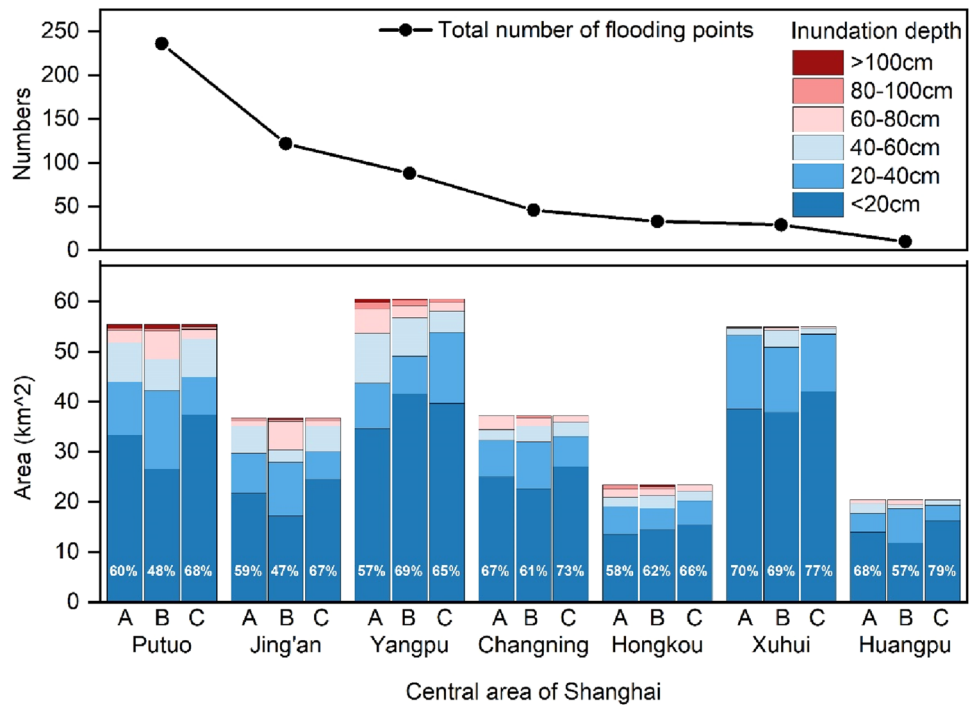


**Table 2** Probabilities of detection (PODs) under different rainfall scenarios during Fitow (2013)

Inundation depth (cm)	A: POD (%)	B: POD (%)	C: POD (%)
> 0	100	100	100
≥ 2	77	80	75
≥ 5	66	67	61

A, B, and C represent scenarios of station observations, radar fusion data, and radar quantitative precipitation estimates (QPE), respectively

radar fusion data can be effectively applied to urban typhoon pluvial flood modeling.

### 3.2 Pluvial Flood Simulation at the Neighborhood Scale

Considering the complex distribution of urban buildings and road network in Shanghai, the detailed features of pluvial flood inundation are better captured with a higher resolution neighborhood-scale simulation. Thus, additional flood simulations at the neighborhood scale are performed with 2 m resolutions. A neighborhood in the city center with sufficient flooding points (from Ganquan Road in the west to Pushan Road in the east, as shown in Fig. 1) is selected as the study area. Furthermore, according to the standards of inundation depths in Table 1, the actual inundation depth can be obtained. Figure 6 displays observed flooding points and pluvial flood inundation maps under the three rainfall scenarios during Fitow. For

the central-western region of the study area, the inundation extents are similar under the three rainfall scenarios, which generally coincide with the flooding points. In the western part, the inundation depths under the station observation and radar fusion data scenarios (Fig. 6a, b) are slightly higher than those under the QPE scenario (Fig. 6c). Nevertheless, due to the lack of weather stations (or interpolation error), there is a blank area in the northeast of the study area in Fig. 6a, while in the other two scenarios (Fig. 6b, c), this area has serious inundations.

In contrast to the simulations at the city scale, pluvial flood simulation at the neighborhood scale with a high-accuracy topographic surface model can effectively improve local inundation simulations and capture high-precision distribution characteristics. As shown in Fig. 6, at the city scale, simulations display largely contiguous inundations. However, at the neighborhood scale, refined inundations can be described. Inundation mainly occurs in the areas between streets and buildings, which is more in line with observed urban typhoon pluvial floods, reflecting the importance of a high-precision grid. In general, limited by the original sparse distribution of weather stations, inundations in the eastern region fail to be captured. Limited by the rainfall estimation ability of the QPE, serious inundations in the northwestern corner are underestimated. Radar fusion data can effectively mitigate problems such as the uneven spatial distribution of stations and an underestimated QPE to better reproduce local inundation in high-precision urban typhoon pluvial flood modeling.

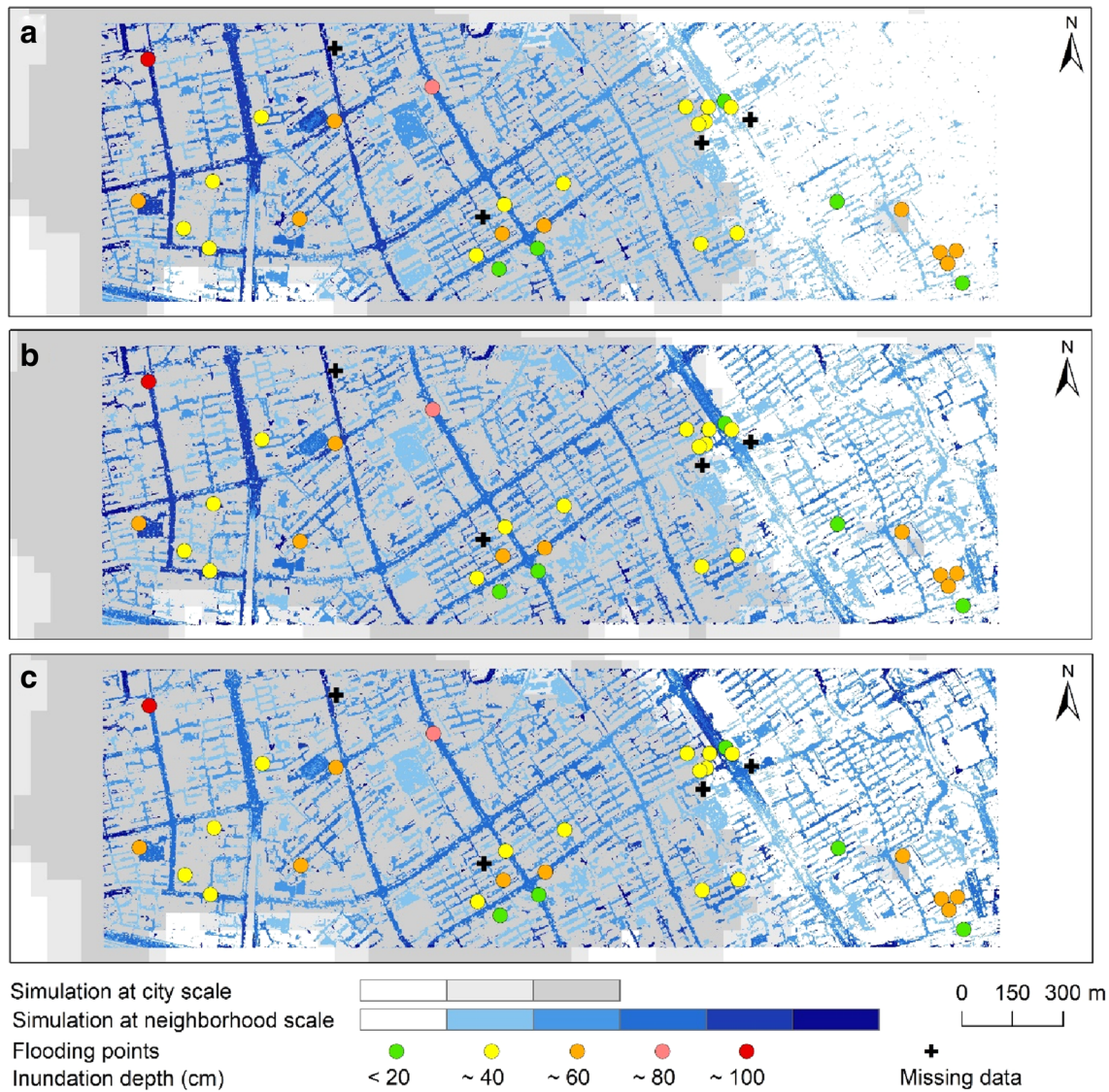


**Fig. 6** Observed flooding points and pluvial flood inundation maps under three rainfall scenarios in the studied neighborhood of Shanghai during Fitow (2013). **a** scenario of station observations; **b** sce-

nario of radar fusion data; **c** scenario of radar quantitative precipitation estimates (QPE)

To quantitatively verify the performance of pluvial flood modeling at the neighborhood scale, a comparison of flooding points and the corresponding modeling results under three rainfall scenarios during Fitow is shown in Fig. 7. The results reveal that, in general, inundation depths under the station observation and radar fusion data scenarios are similar to the observed depths, while the simulations under the QPE scenario are relatively poor. When the depth is below 60 cm, the flood inundation depths under the three scenarios are slightly overestimated. The RMSEs under the station observation and radar fusion data scenarios are 24.21 cm and 26.03 cm, respectively, and that under the QPE scenario is 27.64 cm. There is a systematic deviation of approximately 0–25 cm in the inundation simulations,

but the overall simulations are in good agreement with the observed results. Therefore, generally speaking, in contrast to the QPE, station observations and radar fusion data are more suitable for neighborhood-scale modeling and more consistent with observations.

### 3.3 Temporal Characteristics of Simulated Pluvial Flood

From the perspective of spatial distribution, the above analysis results reveal that the three sets of precipitation data, especially the radar fusion data, can be used in urban pluvial flood modeling. Based on the temporal characteristics of multisource data during pluvial flood progression,

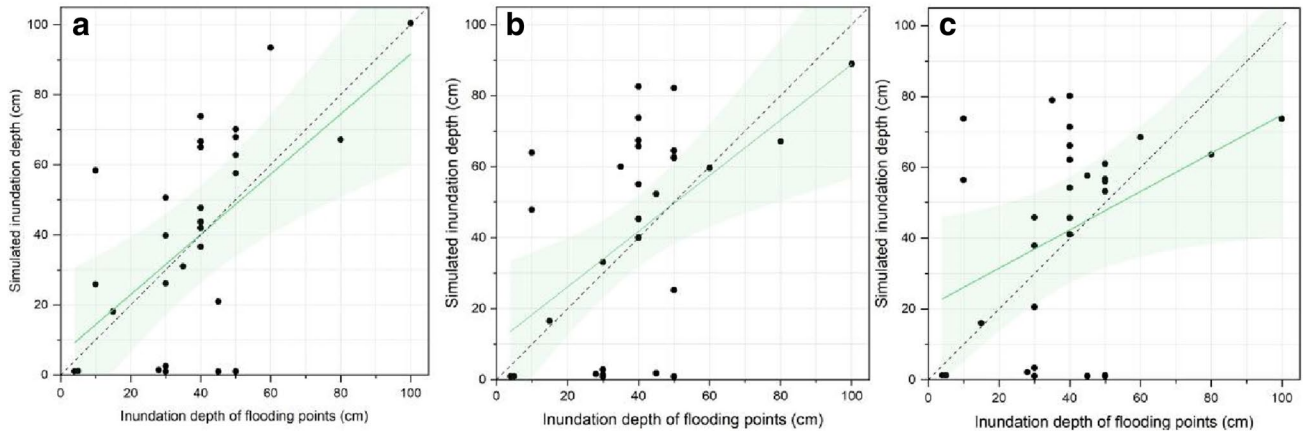
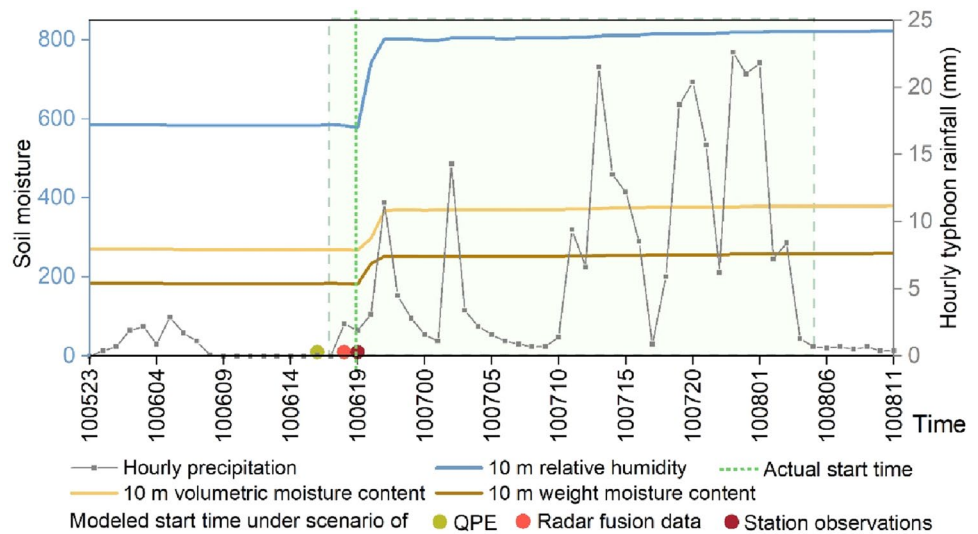


**Fig. 7** A comparison of inundation depth of flooding points and the corresponding modeling results under three rainfall scenarios during Fitow (2013). **a** scenario of station observations; **b** scenario of radar

fusion data; **c** scenario of radar quantitative precipitation estimates (QPE); Green line: linear fitting; dotted line: flooding depths; solid line: best fit of scenario results; Green fill: 95% confidence interval

**Fig. 8** Variation in soil moisture, hourly typhoon rainfall, and inundation depths before and after Fitow (2013). Green fill: periods during Fitow. *QPE* radar quantitative precipitation estimates. The “Time” in the x-axis means month, day, and hour



the impacts of the three precipitation datasets on the accuracy of estimated inundation time are analyzed.

As shown in Fig. 1, a fixed-point to record soil humidity information is located in the southwestern suburb of Shanghai. Using the 1 km radius range of the fixed-point as the study area, we compare the soil humidity before and after the typhoon rainfall and the start time of inundation under the three rainfall scenarios (Fig. 8). The hourly rainfall used in this figure is obtained from the station observation at the fixed-point. Under the three scenarios, the initial times of inundation slightly differ by 1–2 h but generally match the time point at which the soil humidity rises significantly. In other words, the start times of inundation are accurately captured. Subsequently, the rapid increases in the inundation depth and the saturation of soil moisture also indicate the process of continuous flooding under the influence of typhoon rainstorms. As a result, different precipitation data have

little influence on the temporal characteristics of simulated urban typhoon pluvial flood, and all of these data can accurately reflect the occurrence time of floods.

In this study, due to the limitation of fixed-points, the temporal characteristics of the inundation only represent the local area, which may not be applicable to other scales. Therefore, in future work, it is necessary to further enrich soil moisture data, carry out a multiscale study of temporal characteristics, and reveal the influence of multisource precipitation data on estimated inundation time.

### 4 Conclusion

Based on the automatic meteorological station precipitation observations, radar quantitative precipitation

estimates, and radar fusion data during the impact period of the 2013 Typhoon Fitow, pluvial flood modeling is performed at the city, neighborhood, and fixed-point scales using the FloodMap-Hydroinundation2D model. The results obtained are promising and reveal the influence of multisource precipitation data on multiscale urban typhoon pluvial flood modeling.

At the city scale, the simulated inundations (extent and depth) are close to the observed flooding points under the scenarios of station observations and radar fusion data. In contrast, the simulation under the QPE scenario is slightly weaker, especially in regions without heavy rainfall. When the observed inundation depth is above 2 cm, in contrast to the scenario of station observations, the POD under the scenario of radar fusion data can improve by 3%. When the observed inundation depth is above 5 cm, in contrast to the scenario of QPE, the POD under the scenario of radar fusion data can improve by 6%. Therefore, radar fusion data can be effectively applied to urban typhoon pluvial flood modeling.

At the neighborhood scale, pluvial flood simulation with a high-accuracy topographic surface model can effectively improve the local inundation simulation and capture the high-precision distribution characteristics. In contrast to the QPE, station observations and radar fusion data are more suitable for neighborhood-scale modeling. In particular, radar fusion data can effectively mitigate the problems of an uneven spatial distribution of stations and a weak estimation of QPE to accurately capture the details of pluvial floods.

The fixed-point verification shows that the initial times of inundation slightly differ by 1–2 h under the three scenarios but generally match the time point at which the soil humidity rises significantly. Thus, different precipitation data have little influence on the temporal characteristics of simulated urban typhoon pluvial floods.

In addition, urban typhoon pluvial flood modeling is restricted by multiple factors, such as the topography, TC intensity, TC tracks, and urban underlying surface, and thus has a high complexity and uncertainty. To better understand the impacts of typhoon pluvial floods and help policymakers and other concerned stakeholders develop proper measures for urban flood risk management, future research should use the latest data in high-precision urban flood modeling, such as numerical prediction, dual polarization radar data, and assimilation data. Such studies may provide a solid foundation for emergency management of urban typhoon pluvial flood hazards.

**Acknowledgments** This study was sponsored by the National Natural Science Foundation of China (Grant Nos. 41871164, 41806046), the Shanghai Sailing Program (Grant No. 21YF1456900), the Shanghai Philosophy and Social Science Planning Program (Grant No.

2021XRM005), and the Fundamental Research Funds for the Central Universities (Grant No. 2022ECNU-XWK-XK001).

**Open Access** This article is licensed under a Creative Commons Attribution 4.0 International License, which permits use, sharing, adaptation, distribution and reproduction in any medium or format, as long as you give appropriate credit to the original author(s) and the source, provide a link to the Creative Commons licence, and indicate if changes were made. The images or other third party material in this article are included in the article's Creative Commons licence, unless indicated otherwise in a credit line to the material. If material is not included in the article's Creative Commons licence and your intended use is not permitted by statutory regulation or exceeds the permitted use, you will need to obtain permission directly from the copyright holder. To view a copy of this licence, visit <http://creativecommons.org/licenses/by/4.0/>.

## References

- Abro, M.I., D. Zhu, E. Elahi, A.A. Majidano, and B.K. Solangi. 2021. Hydrological simulation using multi-sources precipitation estimates in the Huaihe River Basin. *Arabian Journal of Geosciences* 14(18): Article 1912.
- Bates, P.D., and A.P.J. De Roo. 2000. A simple raster-based model for flood inundation simulation. *Journal of Hydrology* 236(1–2): 54–77.
- Bates, P.D., M.S. Horritt, and T.J. Fewtrell. 2010. A simple inertial formulation of the shallow water equations for efficient two-dimensional flood inundation modelling. *Journal of Hydrology* 387(1–2): 33–45.
- Bisht, D.S., C. Chatterjee, S. Kalakoti, P. Upadhyay, M. Sahoo, and A. Panda. 2016. Modeling urban floods and drainage using SWMM and MIKE URBAN: A case study. *Natural Hazards* 84(2): 749–776.
- Calder, I.R., R.J. Harding, and P.T.W. Rosier. 1983. An objective assessment of soil-moisture deficit models. *Journal of Hydrology* 60(1–4): 329–355.
- Chao, L., K. Zhang, Z.-L. Yang, J. Wang, P. Lin, J. Liang, Z. Li, and Z. Gu. 2021. Improving flood simulation capability of the WRF-hydro-RAPID model using a multi-source precipitation merging method. *Journal of Hydrology* 592: Article 125814.
- Chen, L., Y. Duan, L. Song, and Y. Xu. 2012. *Typhoon forecast and disasters*. Beijing: China Meteorological Press (in Chinese).
- Chen, W., Y. Duan, Y. Lu, J. Fang, X. Shi, and F. Ren. 2017. Review on tropical cyclone risk assessment. *Journal of Catastrophology* 32(4): 146–152 (in Chinese).
- Chen, Y., E.E. Ebert, K.J.E. Walsh, and N.E. Davidson. 2013. Evaluation of TRMM 3B42 precipitation estimates of tropical cyclone rainfall using PACRAIN data. *Journal of Geophysical Research: Atmospheres* 118(5): 2184–2196.
- Ding, Y., G. Ren, and G. Shi. 2006. National assessment report of climate change (I): Climate change in China and its future trend. *Climate Change Research* 2(1): 3–8 (in Chinese).
- Gao, W., H. Chen, and J. Tan. 2017. Application and prospect of urban integrated meteorological observation network in Shanghai. *Advances in Meteorological Science and Technology* 7(6): 99–104 (in Chinese).
- Gigović, L., D. Pamučar, Z. Bajić, and S. Drobniak. 2017. Application of GIS-interval rough AHP methodology for flood hazard mapping in urban areas. *Water* 9(6): Article 360.
- IPCC (Intergovernmental Panel on Climate Change). 2021. *Climate change 2021: The physical science basis; Contribution of Working Group I to the Sixth Assessment Report of the Intergovernmental Panel on Climate Change*, ed. V. Masson-Delmotte, P. Zhai, A.

- Pirani, S.L. Connors, C. Péan, S. Berger, N. Caud, Y. Chen, et al. Cambridge, UK: Cambridge University Press.
- Lai, Y., J. Li, X. Gu, Y. Chen, D. Kong, T. Gan, M. Liu, Q. Li, and G. Wu. 2020. Greater flood risks in response to slowdown of tropical cyclones over the coast of China. *Proceedings of the National Academy of Sciences* 117(26): 14751–14755.
- Li, W., B. Xu, and J. Wen. 2016. Scenario-based community flood risk assessment: A case study of Taining county town, Fujian province, China. *Natural Hazards* 82(1): 193–208.
- Lin, L. 2014. The hydrological effect and threshold effect of impervious area in Shanghai over the last 50 years. Master's thesis, *Shanghai University*, China (in Chinese).
- Ly, S., C. Charles, and A. Degre. 2013. Different methods for spatial interpolation of rainfall data for operational hydrology and hydrological modeling at watershed scale: A review. *Biotechnologie, Agronomie, Société et Environnement* 17(2): 392–406.
- Mosaffa, H., M. Sadeghi, N. Hayatbini, V.A. Gorooh, A.A. Asanjan, P. Nguyen, and S. Sorooshian. 2020. Spatiotemporal variations of precipitation over Iran using the high-resolution and nearly four decades satellite-based PERSIANN-CDR dataset. *Remote Sensing* 12(10): Article 1584.
- Quan, R. 2021. Impact of future land use change on pluvial flood risk based on scenario simulation: A case study in Shanghai, China. *Arabian Journal of Geosciences* 14(11): Article 943.
- Shanghai Typhoon Institute. Chinese Meteorological Administration. 2014. *Yearbook of tropical cyclone in China for 2013*. Beijing: China Meteorological Press (in Chinese).
- Shi, P., J. Du, M. Ji, J. Liu, and J. Wang. 2006. Urban risk assessment research of major natural disasters in China. *Advances in Earth Science* 21(2): 170–177.
- Shi, J., Y. Gu, H. Mu, Q. Wang, and M. Xu. 2014. Development of urban rainstorm and gale disaster chain in Shanghai. *Proceedings of 2014 National Forum on Comprehensive Disaster Prevention*. 82–89. (in Chinese).
- Sirisena, T.A.J.G., S. Maskey, R. Ranasinghe, and M.S. Babel. 2018. Effects of different precipitation inputs on streamflow simulation in the Irrawaddy River Basin, Myanmar. *Journal of Hydrology: Regional Studies* 19: 265–278.
- Song, L., and Z. Xu. 2019. Coupled hydrologic-hydrodynamic model for urban rainstorm water logging. *Journal of Beijing Normal University (Natural Science)* 55(5): 581–587 (in Chinese).
- Tang, Y. 2018. *Study on urban flooding under design and real-time simulation condition based on radar estimation and forecast of rainfall*. Beijing: Beijing University of Technology (in Chinese).
- Wang, K., and A. Altunkaynak. 2012. Comparative case study of rainfall-runoff modeling between SWMM and fuzzy logic approach. *Journal of Hydrologic Engineering* 17(2): 283–291.
- Wang, X., X. Xu, and X. Yang. 2017. The NWP models' evaluation of landfall processes of the strong typhoon Fitow. *Transactions of Atmospheric Sciences* 40(5): 609–618 (in Chinese).
- Wang, X., H. Yu, X. Bao, and L. Bai. 2017. Analysis on extreme characteristics of the precipitation brought by typhoon "Fitow" (1323). *Journal of the Meteorological Sciences* 37(4): 514–521 (in Chinese).
- Wang, J., Y. Zhao, Z. Ren, and J. Gao. 2018. Design and verification of quality control methods for automatic soil moisture observation data in China. *Meteorological Monthly* 44(2): 244–257 (in Chinese).
- Wen, L., K. Zhao, G. Chen, M. Wang, B. Zhou, H. Huang, D. Hu, W.C. Lee, and H. Hu. 2018. Drop size distribution characteristics of seven typhoons in China. *Journal of Geophysical Research: Atmospheres* 123(12): 6529–6548.
- Wu, Y., and W. Wu. 2021. Study on the distribution of extreme precipitation and its potential risks in the middle and lower reaches of the Yangtze River in China. *Fresenius Environmental Bulletin* 30(8): 9986–9992.
- Wu, D., T. Cao, and H. Xue. 2016. The study of quality control for observing data of automatic soil moisture. *Hans Journal of Soil Science* 4(1): 1–10 (in Chinese).
- Wu, X., D. Yu, Z. Chen, and R.L. Wilby. 2012. An evaluation of the impacts of land surface modification, storm sewer development, and rainfall variation on waterlogging risk in Shanghai. *Natural Hazards* 63(2): 305–323.
- Xu, X., Y. Du, J. Tang, and Y. Wang. 2011. Variations of temperature and precipitation extremes in recent two decades over China. *Atmospheric Research* 101(1): 143–154.
- Yin, J., M. Ye, Z. Yin, and S. Xu. 2015. A review of advances in urban flood risk analysis over China. *Stochastic Environmental Research and Risk Assessment* 29(3): 1063–1070.
- Yin, J., D. Yu, and B. Liao. 2020. A city-scale assessment of emergency response accessibility to vulnerable populations and facilities under normal and pluvial flood conditions for Shanghai, China. *Environment and Planning B: Urban Analytics and City Science* 48(8): 2239–2253.
- Yin, J., D. Yu, Z. Yin, M. Liu, and Q. He. 2016. Evaluating the impact and risk of pluvial flash flood on intra-urban road network: A case study in the city center of Shanghai, China. *Journal of Hydrology* 537: 138–145.
- Yin, J., D. Yu, Z. Yin, J. Wang, and S. Xu. 2013. Modelling the combined impacts of sea-level rise and land subsidence on storm tides induced flooding of the Huangpu River in Shanghai, China. *Climatic Change* 119(3–4): 919–932.
- Yoon, S., and B. Lee. 2017. Effects of using high-density rain gauge networks and weather radar data on urban hydrological analyses. *Water* 9(12): Article 931.
- Yu, D., and T.J. Coulthard. 2015. Evaluating the importance of catchment hydrological parameters for urban surface water flood modelling using a simple hydro-inundation model. *Journal of Hydrology* 524: 385–400.
- Zhang, J., and Y. Chen. 2019. Risk assessment of flood disaster induced by typhoon rainstorms in Guangdong province, China. *Sustainability* 11(10): Article 2738.
- Zhang, P., B. Du, and T. Dai. 2001. *Radar meteorology*. Beijing: China Meteorological Press (in Chinese).